
Learning Probabilities of Causation from Finite Population Data

Ang Li, Song Jiang, Yizhou Sun, Judea Pearl
Department of Computer Science
University of California Los Angeles
Los Angeles, CA 90095
{angli, songjiang, yzsun, judea}@cs.ucla.edu

Abstract

This paper deals with the problem of learning the probabilities of causation of subpopulations given finite population data. The tight bounds of three basic probabilities of causation, the probability of necessity and sufficiency (PNS), the probability of sufficiency (PS), and the probability of necessity (PN), were derived by Tian and Pearl. However, obtaining the bounds for each subpopulation requires experimental and observational distributions of each subpopulation, which is usually impractical to estimate given finite population data. We propose a machine learning model that helps to learn the bounds of the probabilities of causation for subpopulations given finite population data. We further show by a simulated study that the machine learning model is able to learn the bounds of PNS for 32768 subpopulations with only knowing roughly 500 of them from the finite population data.

1 Introduction

The probability of causation is a crucial concept that belongs to the third ladder of causality defined by Pearl [19] and plays a significant role in modern decision-making. The applications include the areas of marketing, political science, and health science. For example, using a linear combination of the probabilities of causation, Li and Pearl defined the benefit function of the unit selection problem, which is considered to be a revolution of the traditional A/B test heuristics [9, 11, 13]. Personalized decision-making, for another example, has been demonstrated that it should consider the probabilities of causation [14]. The label of a machine learning algorithm should also combine the probabilities of causation terms to capture the counterfactual behavior of the desired task [10].

Using structural causal model (SCM) [5, 6, 18], Pearl [17] first defined three basic probabilities of causation (i.e., PNS, PN, and PS). These probabilities of causation were then bounded tightly by Tian and Pearl [20] using Balke’s programming [3]. The theoretical proof of those bounds was provided at [11, 13]. After that, researchers started to use covariate information and the causal structure to narrow the bounds of the above probabilities of causation [4, 15]. Li and Pearl [8] also presented extended studies of the probabilities of causation with nonbinary treatment and effect.

All listed works above are focused on providing bounds of the probabilities of causation on a specific population and require the experimental and observational distributions of the population. If the population can be divided into subpopulations by some observed characteristics, then the estimations of the probabilities of causation for each subpopulation require the experimental and observational distributions of each subpopulation. Consider the following example: an online music provider wants to increase its user subscription rate by sending gifts to new subscribers. Therefore, based on customer characteristics such as income, age, and usage, the company wants to identify customers who are likely to subscribe if and only if they received the gift. The gifts are value earphones; thus,

the music provider prefers that these gifts be made only to those identified customers. Therefore, the music provider wants to know which kind of characteristics contains more desired customers. The quantities that the music provider wanted are then the PNS of subpopulations for each set of customer characteristics. If we want to apply Tian-Pearl’s PNS bounds [20], we need the experimental and observational distributions of each set of customer characteristics. However, the data available are usually finite many for the whole population; therefore, 1) it is impractical to estimate each distribution because the number of subpopulations is large; 2) some of the subpopulations are very rare (i.e., they appeared with a low probability) or even with no data associated; 3) we are not able to forecast the new coming subpopulations.

In this work, we are considering binary treatment and effect and will focus on PNS. It is not hard to extend to the other probabilities of causation. We also classify individual behavior into four response types, labeled complier, always-taker, never-taker, and defier [1, 2, 11]. Compliers are individuals who would respond positively if encouraged and negatively if not encouraged (i.e., PNS is the fraction of compliers). Always-takers are individuals who always respond positively whether or not they are encouraged. Never-takers are individuals who always respond negatively whether or not they are encouraged. Defiers are individuals who would respond negatively if encouraged and positively if not encouraged. We assume that the response type of an individual is determined by his characteristics (observed or unobserved characteristics); therefore, we propose a machine learning framework that is able to output the lower and upper bounds of PNS for each subpopulation given finite population data (i.e., learn the relations between the characteristics and the response types).

2 Preliminaries

Here, the definitions of three basic probabilities of causation are reviewed [17]. We follow the language of counterfactuals in structural causal model in [5, 6].

We use $Y_x = y$ to denote the basic counterfactual sentence “Variable Y would have the value y , had X been x ”. If not specified, we use y_x to denote $Y_x = y$, X stands for treatment, and Y stands for effect. The experimental distributions in this paper are those in the form of the causal effects, $P(y_x)$, and the observational distributions in this paper are those joint probability function $P(x, y)$.

Three basic probabilities of causation are defined as follows:

Definition 1 (Probability of necessity (PN)). *Let X and Y be two binary variables in a causal model M , let x and y stand for the propositions $X = \text{true}$ and $Y = \text{true}$, respectively, and x' and y' for their complements. The probability of necessity is defined as the expression [17]*

$$\begin{aligned} PN &\triangleq P(Y_{x'} = \text{false} | X = \text{true}, Y = \text{true}) \\ &\triangleq P(y'_{x'} | x, y) \end{aligned}$$

Definition 2 (Probability of sufficiency (PS)). [17]

$$PS \triangleq P(y_x | y', x')$$

Definition 3 (Probability of necessity and sufficiency (PNS)). [17]

$$PNS \triangleq P(y_x, y'_{x'})$$

PNS stands for the probability that y would respond to x both ways, and therefore measures both the sufficiency and necessity of x to produce y .

The tight bounds of PNS, PN and PS derived by Tian and Pearl [20] are then in the following forms:

$$\max \left\{ \begin{array}{l} 0, \\ P(y_x) - P(y_{x'}), \\ P(y) - P(y_{x'}), \\ P(y_x) - P(y) \end{array} \right\} \leq \text{PNS} \leq \min \left\{ \begin{array}{l} P(y_x), \\ P(y'_{x'}), \\ P(x, y) + P(x', y'), \\ P(y_x) - P(y_{x'}) + P(x, y') + P(x', y) \end{array} \right\} \quad (1)$$

$$\max \left\{ \begin{array}{l} 0, \\ \frac{P(y) - P(y_{x'})}{P(x, y)} \end{array} \right\} \leq \text{PN} \leq \min \left\{ \begin{array}{l} 1, \\ \frac{P(y'_{x'}) - P(x', y')}{P(x, y)} \end{array} \right\}$$

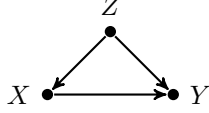


Figure 1: The Causal Model, where X , Y and Z are binary treatment, binary effect, and 20 independent binary features, respectively.

$$\max \left\{ \frac{0, P(y') - P(y_x)}{P(x', y')} \right\} \leq \text{PS} \leq \min \left\{ \frac{1, P(y_x) - P(x, y)}{P(x', y')} \right\}$$

To obtain bounds for a specific subpopulation, defined by a set C of characteristics, the expressions above should be modified by conditioning each term on $C = c$. Therefore, if the experimental and observational distributions are available for every subpopulation, we are able to estimate the probabilities of causation of every subpopulation (here, we reviewed Tian-Pearl bounds for PNS, PS, and PN; Li and Pearl provided bounds for all types of probabilities of causation in [8]). However, in practice, some subpopulations have no adequate data (due to finite population data) to estimate their experimental and observational distributions. In this paper, we propose a machine learning model that takes the bounds of the probabilities of causation (i.e., those bounds that have adequate data to estimate) as the label and provides the estimations of the probabilities of causation of all rest subpopulations.

3 Causal Model

In order to verify the accuracy of the learned bounds of PNS, we must first understand the data generating process to have the true PNS value and its bounds. The model we are using is shown in Figure 1 (the coefficients in SCM are randomly generated as in [7], see the appendix for the detail), where X is a binary treatment, Y is a binary effect, and Z is a set of 20 independent binary features (say Z_1, \dots, Z_{20}). The structural equations are as follow (for simplicity reason, we let $x = 1, x' = 0$, and $y = 1, y' = 0$):

$$\begin{aligned} Z_i &= U_{Z_i} \text{ for } i \in \{1, \dots, 20\}, \\ X &= f_X(M_X, U_X) = \begin{cases} 1 & \text{if } M_X + U_X > 0.5, \\ 0 & \text{otherwise,} \end{cases} \\ Y &= f_Y(X, M_Y, U_Y) = \begin{cases} 1 & \text{if } 0 < CX + M_Y + U_Y < 1 \\ 1 & \text{if } 1 < CX + M_Y + U_Y < 2, \\ 0 & \text{otherwise,} \end{cases} \end{aligned}$$

where, U_{Z_i}, U_X, U_Y are binary exogenous variables with Bernoulli distributions, C is a constant, and M_X, M_Y are linear combinations of Z_1, \dots, Z_{20} .

The value of C, M_X, M_Y and the distributions of $U_X, U_Y, U_{Z_1}, \dots, U_{Z_{20}}$ for the model are provided in the appendix.

4 Data Generating Process

Based on the model defined in the last section, there are 20 binary features. We made 15 of them observable and 5 of them unobservable. All exogenous variables are also made unobservable. We then have 2^{15} observed subpopulations.

4.1 Informer Data

The informer data must know the actual bounds of PNS of each subpopulation for comparison purposes. From the structural equation given in last section, the value of X is determined by U_X

and M_x (denoted by $f_X(M_X, U_X)$) and the value of Y is determined by X , M_Y , and U_Y (denoted by $f_Y(X, M_Y, U_Y)$). If all 20 binary features are observable, then for a particular features $z = (z_1, \dots, z_{20})$, M_X and M_Y are fixed (denoted by $M_X(z)$ and $M_Y(z)$), then the PNS, experimental distribution, and observational distribution of this set of features are

$$\begin{aligned}
PNS(z) &= P(Y = 0_{X=0}, Y = 1_{X=1} | z) \\
&= P(U_Y = 0) * T_0 + P(U_Y = 1) * T_1, \\
\text{where, } T_0 &= \left\{ \begin{array}{ll} 1 & \text{if } Y(0, M_Y(z), 0) = 0 \text{ and } Y(1, M_Y(z), 0) = 1, \\ 0 & \text{otherwise,} \end{array} \right\}, \\
T_1 &= \left\{ \begin{array}{ll} 1 & \text{if } Y(0, M_Y(z), 1) = 0 \text{ and } Y(1, M_Y(z), 1) = 1, \\ 0 & \text{otherwise} \end{array} \right\}. \\
P(Y = 1 | do(X), z) \\
&= P(U_Y = 0) * Y(X, M_Y(z), 0) + P(U_Y = 1) * Y(X, M_Y(z), 1). \\
P(Y = 1 | X, z) \\
&= P(U_X = 0) * P(U_Y = 0) * Y(X(M_X(z), 0), M_Y(z), 0) + \\
&\quad P(U_X = 0) * P(U_Y = 1) * Y(X(M_X(z), 0), M_Y(z), 1) + \\
&\quad P(U_X = 1) * P(U_Y = 0) * Y(X(M_X(z), 1), M_Y(z), 0) + \\
&\quad P(U_X = 1) * P(U_Y = 1) * Y(X(M_X(z), 1), M_Y(z), 1).
\end{aligned}$$

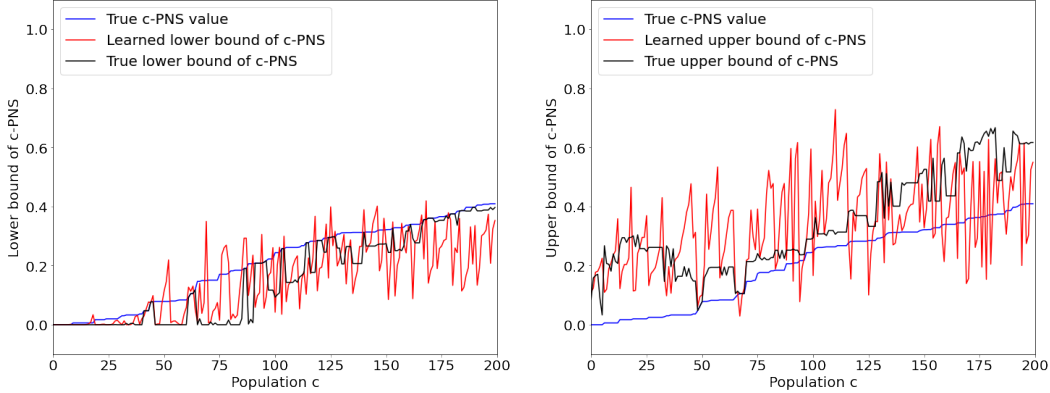
We assumed 15 of the features are observable (say Z_1, \dots, Z_{15}), which means each subpopulation $c = (z_1, \dots, z_{15})$ consists 32 sets of 20 binary features (say $s_0 = (z_1, \dots, z_{15}, 0, 0, 0, 0, 0)$, $s_1 = (z_1, \dots, z_{15}, 0, 0, 0, 0, 1)$, $s_2 = (z_1, \dots, z_{15}, 0, 0, 0, 1, 0)$, ..., $s_{31} = (z_1, \dots, z_{15}, 1, 1, 1, 1, 1)$), then we have the PNS, experimental distribution, and observational distribution of all observed subpopulations are as follow:

$$\begin{aligned}
PNS(c) &= P(Y = 0_{X=0}, Y = 1_{X=1} | c) \\
&= P(s_0)/P(c)PNS(s_0) + P(s_1)/P(c)PNS(s_1) + \\
&\quad P(s_2)/P(c)PNS(s_2) + \dots + P(s_{31})/P(c)PNS(s_{31}) \\
&= P(Z_{16} = 0)P(Z_{17} = 0)P(Z_{18} = 0)P(Z_{19} = 0)P(Z_{20} = 0)PNS(s_0) + \\
&\quad P(Z_{16} = 0)P(Z_{17} = 0)P(Z_{18} = 0)P(Z_{19} = 0)P(Z_{20} = 1)PNS(s_1) + \dots + \\
&\quad P(Z_{16} = 1)P(Z_{17} = 1)P(Z_{18} = 1)P(Z_{19} = 1)P(Z_{20} = 1)PNS(s_{31}). \\
P(Y = 1 | do(X), c) \\
&= P(Z_{16} = 0)P(Z_{17} = 0)P(Z_{18} = 0)P(Z_{19} = 0)P(Z_{20} = 0)P(Y = 1 | do(X), s_0) + \\
&\quad P(Z_{16} = 0)P(Z_{17} = 0)P(Z_{18} = 0)P(Z_{19} = 0)P(Z_{20} = 1)P(Y = 1 | do(X), s_1) + \\
&\quad P(Z_{16} = 0)P(Z_{17} = 0)P(Z_{18} = 0)P(Z_{19} = 1)P(Z_{20} = 0)P(Y = 1 | do(X), s_2) + \dots + \\
&\quad P(Z_{16} = 1)P(Z_{17} = 1)P(Z_{18} = 1)P(Z_{19} = 1)P(Z_{20} = 1)P(Y = 1 | do(X), s_{31}). \\
P(Y = 1 | X, c) \\
&= P(Z_{16} = 0)P(Z_{17} = 0)P(Z_{18} = 0)P(Z_{19} = 0)P(Z_{20} = 0)P(Y = 1 | X, s_0) + \\
&\quad P(Z_{16} = 0)P(Z_{17} = 0)P(Z_{18} = 0)P(Z_{19} = 0)P(Z_{20} = 1)P(Y = 1 | X, s_1) + \\
&\quad P(Z_{16} = 0)P(Z_{17} = 0)P(Z_{18} = 0)P(Z_{19} = 1)P(Z_{20} = 0)P(Y = 1 | X, s_2) + \dots + \\
&\quad P(Z_{16} = 1)P(Z_{17} = 1)P(Z_{18} = 1)P(Z_{19} = 1)P(Z_{20} = 1)P(Y = 1 | X, s_{31}).
\end{aligned}$$

The informer view of the bounds of $PNS(c)$ (i.e., true bounds) could be obtained using Equation 1 and above observational and experimental distributions.

4.2 Experimental Sample

Here is how we collected 5000000 experimental samples for training purposes. From the causal model in Section 3, an individual is determined by U_X , U_Y , and $U_{Z_1}, \dots, U_{Z_{20}}$. Therefore, we first randomly generated $(U_X, U_Y, U_{Z_1}, \dots, U_{Z_{20}})$ using their distributions; then we randomly generated X using *Bernoulli*(0.5); the value of Y is then $f_Y(X, M_Y, U_Y)$. We then obtained a experimental sample, $(U_{Z_1}, U_{Z_2}, \dots, U_{Z_{15}}, X, Y)$ (since 15 features are observable and identical to U_{Z_i}).



(a) Lower bound of the PNS for subpopulations. These 200 subpopulations are randomly selected from 32768 subpopulations.

(b) Upper bound of the PNS for subpopulations. These 200 subpopulations are randomly selected from 32768 subpopulations.

Figure 2: The learned bounds of PNS for subpopulations compared to the true bounds of PNS.

4.3 Observational Sample

Here is how we collected the 5000000 observational samples for training purposes. Similarly to experimental data, we first randomly generated $(U_X, U_Y, U_{Z_1}, \dots, U_{Z_{20}})$ using their distributions; the value of X is then $f_X(M_X, U_X)$; the value of Y is then $f_Y(X, M_Y, U_Y)$. We then collect a observational sample, $(U_{Z_1}, U_{Z_2}, \dots, U_{Z_{15}}, X, Y)$ (since 15 features are observable and identical to U_{Z_i}).

5 Machine Learning Model

5.1 Features and Label

The training features are 15 observed features. We obtain the training label as follows: if a given set of features appeared more than 1300 times (note we use the number 1300 to have a precise estimation of PNS suggested by Li, Mao, and Pearl [7]) in those 5000000 experimental samples and appeared more than 1300 times in those 5000000 observational samples, Frequentist will be used to estimate the experimental and observational distributions. We will then apply Equation 1 to obtain lower bound and upper bound for this set of features (lower bound and upper bound are the labels). We totally have 529 set of features of both lower and upper bounds for training purposes. The 529 sets of features are then split into 423 for the training set and 106 for the testing set.

5.2 Learning

We used a simple fully-connected neural network to predict the lower and upper bounds from the feature set. Specifically, we use four multilayer perceptron (MLP) layers. ReLU is used for activation in the leading three layers while Sigmoid function is used for the output layer. We set the embeddings dimension as 128 for all layers, and train the model for 600 iterations with learning rate 0.01. Our experiments are done at an AWS p3.2xlarge instance.

6 Experimental Results

We randomly selected 200 subpopulations (among 32768) and compared their learned bounds of PNS with the true bounds of PNS computed from the informer data. The results are shown in Figure 2. The learned bounds of PNS for subpopulations are a good fit for the true PNS bounds. The average error of the learned lower bound among 32768 subpopulations is 0.0775, and the average error of the learned upper bound among 32768 subpopulations is 0.1371. They are both acceptable errors given we have only 423 training size to learn 32768 subpopulations.

7 Discussion

We demonstrated that the probabilities of causation for subpopulations could be learned from finite population data. However, we must discuss some properties of our proposed method further.

First, we applied the machine learning model to learn the bounds of PNS in this paper. This method can be applied to any probability of causation. Machine learning provides the ability to learn the probabilities of causation of subpopulations such that there is insufficient data to estimate the experimental and observational distributions. However, the key is that the label of the machine learning model should be the bounds of the probabilities of causation rather than experimental and observational data. Therefore, the size of the training set is no longer 5000000 observational and experimental samples; it is the observational and experimental distributions and the bounds obtained from the distributions (in the example we had in the last section, our training data set are the size of 529).

Second, we applied the simplest machine learning model. However, the key is the framework we proposed. The data generating process is also available; this is the first publicly available data generating process that can test approaches for counterfactual learning. Researchers who are familiar with fancy machine learning models are welcome to apply other machine learning models to this dataset.

Third, this work can be extended to unit selection problems [9, 11] because the unit selection problems are a linear combination of the probabilities of causation. One can also apply this machine learning framework to predict the experimental distributions [12, 16] using observational data.

8 Conclusion

We demonstrated how to obtain bounds of probabilities of causation for subpopulations using finite population data. We proposed a machine learning framework to deliver reasonable estimations. Experiments showed that the probabilities of causation defined by SCM are learnable with proper labels. Data-generating processes are also available for future machine learning models.

Acknowledgements

This research was supported in parts by grants from the National Science Foundation [#IIS-2106908 and #IIS-2231798], Office of Naval Research [#N00014-21-1-2351], and Toyota Research Institute of North America [#PO-000897].

References

- [1] Joshua D Angrist, Guido W Imbens, and Donald B Rubin. Identification of causal effects using instrumental variables. *Journal of the American statistical Association*, 91(434):444–455, 1996.
- [2] Alexander Balke and Judea Pearl. Bounds on treatment effects from studies with imperfect compliance. *Journal of the American Statistical Association*, 92(439):1171–1176, 1997.
- [3] Alexander Abraham Balke. *Probabilistic counterfactuals: semantics, computation, and applications*. University of California, Los Angeles, 1995.
- [4] Philip Dawid, Monica Musio, and Rossella Murtas. The probability of causation. *Law, Probability and Risk*, (16):163–179, 2017.
- [5] David Galles and Judea Pearl. An axiomatic characterization of causal counterfactuals. *Foundations of Science*, 3(1):151–182, 1998.
- [6] Joseph Y Halpern. Axiomatizing causal reasoning. *Journal of Artificial Intelligence Research*, 12:317–337, 2000.
- [7] A. Li, R. Mao, and J. Pearl. Probabilities of causation: Adequate size of experimental and observational samples. Technical Report R-518, <http://ftp.cs.ucla.edu/pub/stat_ser/r518.pdf>, Department of Computer Science, University of California, Los Angeles, CA, 2022.

- [8] A. Li and J. Pearl. Probabilities of causation with non-binary treatment and effect. Technical Report R-516, Department of Computer Science, University of California, Los Angeles, CA, 2022.
- [9] A. Li and J. Pearl. Unit selection with nonbinary treatment and effect. Technical Report R-517, <http://ftp.cs.ucla.edu/pub/stat_ser/r517.pdf>, Department of Computer Science, University of California, Los Angeles, CA, 2022.
- [10] Ang Li, Suming J. Chen, Jingzheng Qin, and Zhen Qin. Training machine learning models with causal logic. In *Companion Proceedings of the Web Conference 2020*, pages 557–561, 2020.
- [11] Ang Li and Judea Pearl. Unit selection based on counterfactual logic. In *Proceedings of the Twenty-Eighth International Joint Conference on Artificial Intelligence, IJCAI-19*, pages 1793–1799. International Joint Conferences on Artificial Intelligence Organization, 7 2019.
- [12] Ang Li and Judea Pearl. Bounds on causal effects and application to high dimensional data. In *Proceedings of the AAAI Conference on Artificial Intelligence*, volume 36, pages 5773–5780, 2022.
- [13] Ang Li and Judea Pearl. Unit selection with causal diagram. In *Proceedings of the AAAI Conference on Artificial Intelligence*, volume 36, pages 5765–5772, 2022.
- [14] Mueller and Pearl. Personalized decision making – a conceptual introduction. Technical Report R-513, Department of Computer Science, University of California, Los Angeles, CA, 2022.
- [15] S. Mueller, A. Li, and J. Pearl. Causes of effects: Learning individual responses from population data. Technical Report R-505, <http://ftp.cs.ucla.edu/pub/stat_ser/r505.pdf>, Department of Computer Science, University of California, Los Angeles, CA, 2021. Forthcoming, Proceedings of IJCAI-2022.
- [16] Judea Pearl. Causal diagrams for empirical research. *Biometrika*, 82(4):669–688, 1995.
- [17] Judea Pearl. Probabilities of causation: Three counterfactual interpretations and their identification. *Synthese*, pages 93–149, 1999.
- [18] Judea Pearl. *Causality*. Cambridge university press, 2nd edition, 2009.
- [19] Judea Pearl and Dana Mackenzie. *The book of why: the new science of cause and effect*. Basic books, 2018.
- [20] Jin Tian and Judea Pearl. Probabilities of causation: Bounds and identification. *Annals of Mathematics and Artificial Intelligence*, 28(1-4):287–313, 2000.

A Appendix

A.1 The Causal Model

The first model in [7] are used where the coefficients for M_X , M_Y and C were uniformly generated from $[-1, 1]$, and the Bernoulli distribution parameters were uniformly generated from $[0, 1]$. The detailed model is as follows:

$$\begin{aligned}
 Z_i &= U_{Z_i} \text{ for } i \in \{1, \dots, 20\}, \\
 X &= f_X(M_X, U_X) = \begin{cases} 1 & \text{if } M_X + U_X > 0.5, \\ 0 & \text{otherwise,} \end{cases} \\
 Y &= f_Y(X, M_Y, U_Y) = \begin{cases} 1 & \text{if } 0 < CX + M_Y + U_Y < 1 \text{ or } 1 < CX + M_Y + U_Y < 2, \\ 0 & \text{otherwise,} \end{cases}
 \end{aligned}$$

where, U_{Z_i}, U_X, U_Y are binary exogenous variables with Bernoulli distributions.s.t.,

$$\begin{aligned}
 U_{Z_1} &\sim \text{Bernoulli}(0.352913861526), U_{Z_2} \sim \text{Bernoulli}(0.460995855543), \\
 U_{Z_3} &\sim \text{Bernoulli}(0.331702473392), U_{Z_4} \sim \text{Bernoulli}(0.885505026779), \\
 U_{Z_5} &\sim \text{Bernoulli}(0.017026872706), U_{Z_6} \sim \text{Bernoulli}(0.380772701708), \\
 U_{Z_7} &\sim \text{Bernoulli}(0.028092602705), U_{Z_8} \sim \text{Bernoulli}(0.220819399962), \\
 U_{Z_9} &\sim \text{Bernoulli}(0.617742227477), U_{Z_{10}} \sim \text{Bernoulli}(0.981975046713), \\
 U_{Z_{11}} &\sim \text{Bernoulli}(0.142042291381), U_{Z_{12}} \sim \text{Bernoulli}(0.833602592350), \\
 U_{Z_{13}} &\sim \text{Bernoulli}(0.882938907115), U_{Z_{14}} \sim \text{Bernoulli}(0.542143191999), \\
 U_{Z_{15}} &\sim \text{Bernoulli}(0.085023436884), U_{Z_{16}} \sim \text{Bernoulli}(0.645357252864), \\
 U_{Z_{17}} &\sim \text{Bernoulli}(0.863787135134), U_{Z_{18}} \sim \text{Bernoulli}(0.460539711624), \\
 U_{Z_{19}} &\sim \text{Bernoulli}(0.314014079207), U_{Z_{20}} \sim \text{Bernoulli}(0.685879388218), \\
 U_X &\sim \text{Bernoulli}(0.601680857267), U_Y \sim \text{Bernoulli}(0.497668975278), \\
 C &= -0.77953605542,
 \end{aligned}$$

$$M_X = [Z_1 \ Z_2 \ \dots \ Z_{20}] \times \begin{bmatrix} 0.259223510143 \\ -0.658140989167 \\ -0.75025831768 \\ 0.162906462426 \\ 0.652023463285 \\ -0.0892939586541 \\ 0.421469107769 \\ -0.443129684766 \\ 0.802624388789 \\ -0.225740978499 \\ 0.716621631717 \\ 0.0650682260309 \\ -0.220690334026 \\ 0.156355773665 \\ -0.50693672491 \\ -0.707060278115 \\ 0.418812816935 \\ -0.0822118703986 \\ 0.769299853833 \\ -0.511585391002 \end{bmatrix}, M_Y = [Z_1 \ Z_2 \ \dots \ Z_{20}] \times \begin{bmatrix} -0.792867111918 \\ 0.759967136147 \\ 0.55437722369 \\ 0.503970540409 \\ -0.527187144651 \\ 0.378619988091 \\ 0.269255196301 \\ 0.671597043594 \\ 0.396010142274 \\ 0.325228576643 \\ 0.657808327574 \\ 0.801655023993 \\ 0.0907679484097 \\ -0.0713852594543 \\ -0.0691046005285 \\ -0.222582013343 \\ -0.848408031595 \\ -0.584285069026 \\ -0.324874831799 \\ 0.625621583197 \end{bmatrix}$$